HUMAN HEALTH & HALAL METRICS

Research article

Journal of Human, Health and Halal Metrics; 2020, 1(1): 8-20
https://doi.org/10.30502/JHHHM.2020.107918

Fabrication of a novel bio-adsorbent based on the yellow membrane of chicken feet for cationic dye of methylene blue removal: adsorption, equilibrium, kinetic and thermodynamic studies

Samaneh Farrokhzadeh[1*], Habib Razmi[1], Naficeh Sadeghi[2], Elnaz Marzi Khosrowshahi[3]

1- Analytical Chemistry Research Lab, Faculty of Basic Sciences, Azarbaijan Shahid Madani University, Tabriz, Iran.
2- Department of Drug and Food Control, School of Pharmacy, Tehran University of Medical Sciences, Tehran, Iran.
3- Department of Analytical Chemistry, Faculty of Chemistry, Tabriz University, Tabriz, Iran.

Submission: 22 February 2020 ***Revision***: 23 February 2020 ***Acceptance***: 09 March 2020

Abstract

Background and objective: Dye molecules as an important type of organic pollutants are potentially toxic and have carcinogenic and mutagenic impact on living systems. Today, uncontrolled discharge of organic pollutants is environmental problem. Dissolution of synthetic dyes in aqueous media causes decreased light penetration into water and interferes photosynthesis reactions. In the current work, we fabricated a novel and biodegradable adsorbent by chicken feet yellow membrane (CFYM) for removal of cationic dye.

Materials and methods: Untreated CFYM was collected from slaughterhouse and prepared for analysis after washing by deionized water, drying at 90°C for 12-24 h and grinding to fine powders. The adsorbent was instrumentally characterized by Fourier transform infrared spectroscopy, X-ray diffraction, Scanning electron microscopy, and Emmett and Teller techniques. Functional groups of C=O, O–H, N–H, C–N, C–C and H–C–H showed that the pre-treated CFYM mainly contained organic compounds. Removability and efficiency of bio-adsorbent were studied using cationic methylene blue (MB) as s model. For optimization, main variables of pH, adsorbent mass, contact time and temperature were studied by one-factor-at-a-time method through adsorption experiments in a batch system. The equilibrium adsorption experiments were evaluated by Langmuir, Freundlich, Tempkin and Dubinin-Raduskovich isotherm models. The adsorption kinetic models of pseudo-first order, second first order, Elovich and intra-particle diffusion were also studied.

Results and conclusion: Results were in accordance to Langmuir isotherm model. Obtained kinetic and thermodynamic parameters confirmed that pseudo-first order model was the best kinetic model and adsorption process of MB on CFYM was exothermic and spontaneous. Based on the results, CFYM, as a novel natural adsorbent, was efficient for removal of cationic organic pollutant from aqueous solutions.

Keywords: Chicken feet yellow membrane, isotherm; kinetic, Methylene blue, removal

*Correspondence to: Samaneh Farrokhzadeh; e-mail: Samanehfarrokhzadeh@azaruniv.ac.ir; Tel.: +98-4134327500; Fax: +98-4134327541

1. Introduction

In recent years, some methods were used to remove contaminants in environmental systems. In general, these methods are into three groups of physical, chemical and biological including chemical oxidation, coagulation, ion exchange, electrochemical, photochemical, reverse osmosis and adsorption process [1–4]. Adsorption-based method is one of the most convenient techniques for this purpose because of its simplicity, easy operation, compatibility with a variety of pollutants, degradability, reusability and low cost [5]. Up to date, this method has been utilized different adsorbent materials such as activated carbon [6], carbon nanotube [7], iron oxide [8], polymers [9] and molecular sieves [10]. Most synthetic and chemical adsorbents are unavailable, expensive, non-ecofriendly and might include complex synthetic process. Therefore, it is important to examine available and economical adsorbents in practice. Cost-effective adsorbents for water treatment and waste management include natural materials, agricultural by-products [11-13], industrials wastes [14], biomass materials [15] and biomass-based activated carbons [16] which were used for removal of various types of dyes. In this regard, chicken feet yellow membrane (CFYM) is safe and easy-prepared, cost-effective, biodegradable, and available that highlights it over chemical adsorbents. Therefore, main goal of present work is fabrication of a novel, available and inexpensive natural adsorbent based on CFYM as an organic bio-waste for removal of methylene blue (MB) from aqueous environments [17]. MB was selected as model because it is usually found in effluents of textile factories and may cause health concern [18].

2. Materials and methods

2.1. Chemicals

MB, Sodium hydroxide and hydrochloric acid were purchased from Merck (Darmstadt, Germany). Stock solution of MB was prepared at concentration of 1000 mg l^{-1}.

2.2. Preparation of bio-adsorbent powder

CFYM wastes were prepared from hen slaughterhouse (Tehran, Iran). Approximately, 20 g of CFYM was rinsed by hot deionized water repeatedly to remove the fat content. Then, yellow membrane was dried in oven at 95°C for 24 h. The membrane was further powdered. Finally, it was washed with deionized water and dried in oven at 90°C for 12 h before use.

2.3. Characterization

CFYM was characterized by analytical techniques. The microstructure was analyzed by scanning electron microscope (SEM) model Mira 3 Tescan (TESCAN Electron Microscopy Inc., Brno-Czech Republic) [19]. X-ray diffraction (XRD) analysis was followed by Bruker D8 Advance instrument (Bruker AXS, Karlsruhe, Germany) with Cu-Kα radiation source generated at 40.0 kV and 35.0 mA under ambient temperature [19]. Fourier transform infrared (FT-IR) spectra was achieved by FT-IR spectrometer (Bruker, Ettlingen, Germany) [19]. Brunauer, Emmett and Teller (BET) method with Gemini 2375 micrometric apparatus analyzed the specific surface area and pore volume of CFYM. The powdered biomass was degassed at 100ºC at first and experiments were conducted by N_2 adsorption-desorption method [20]. The bio-adsorbent particles were removed from liquid phase by centrifugation at 958 ×g for 15 min. Absorption experiments were carried out by UV-VIS spectrophotometer model T80 (Unico, USA).

2.4. Optimization of effective variables

Experimental design was carried out based on one-factor-at-a-time approach. In this regard, five variables of pH, absorbent mass, contact time, dye concentration and temperature were analyzed. Each time, one variable was studied within a common range that used in other studies and other four variables were constant. At the end, optimum points of variables were followed for characterization of adsorbent-dye interaction in current study. To study influence of pH on adsorption process, MB dye solutions at 50 mg l^{-1}

concentration were prepared at different pH ranged from 2 to 12 and absorption was read at 665 nm. Then, 100 mg of the adsorbent was added to solutions. Absorption of final solution was read by spectrophotometer at 665 nm. Similar experiments were done in range of 10-200 mg for absorbent mass, 10-125 min for contact time, 10-100 mg l^{-1} for dye concentration and 20, 30, 50, 70°C for temperature.

2.5. Analytical and efficacy experiments

To find the optimum wavelength at spectro-photometer, UV-VIS spectra of different concentrations of MB (10-100 mg l^{-1}) were recorded in range of 200-900 nm and optimum wavelength of 665 nm was achieved. Therefore, average concentration and 665 nm wavelength were selected for further experiments. All data analysis was performed by Excel software. The adsorption tests of MB on CFYM was performed through a batch operational system. At the end of each experiment, 3 ml of solution was centrifuged at 958 ×g for 15 min. Concentration of residual dye in supernatant was detected using UV-VIS spectrometer at λ_{max} of 665 nm. Removal efficiency of bio-adsorbent (R%) and the amount of adsorbed dye on the adsorbent at equilibrium (q_e: mg g^{-1}), were calculated as follows (Eq. 1 and 2):

$$R(\%) = \frac{(C_0 - C_e)}{C_0} \times 100 \qquad \text{Eq. 1}$$

$$q_e = \frac{(C_0 - C_e)V}{m} \qquad \text{Eq. 2}$$

Where, C_o and C_e are initial and equilibrium dye concentrations (mg l^{-1}) respectively, m is adsorbent mass (g) and V is volume of solution.

3. Results and discussion

3.1. Characterization of bio-adsorbent

In Figure 1, the FT-IR peak at 1239 cm^{-1} is related to stretching C–N of aliphatic amines, wagging C–H of alkyl halides and stretching C–O of carboxylic acids [20]. CH_2 bending vibrations of alkanes (carbohydrates) and C–C stretching vibrations of aromatic groups in structure are detected at 1458 cm^{-1}. Furthermore, observed peaks at 1542 and 1654 cm^{-1} are related to amide II (from an out-of-phase combination of N–H in-plane bending and C–N stretching vibrations of peptide linkages) and amide I (C=O stretching vibration with minor contribution of C–N stretch), respectively. The peaks at 2853 and 2924 cm^{-1} are related to CH_2 symmetric stretch vibrations of amide phases of collagen part. The band between 3200–3500 cm^{-1} is due to O–H and N–H stretch vibrations in amide structures [21].

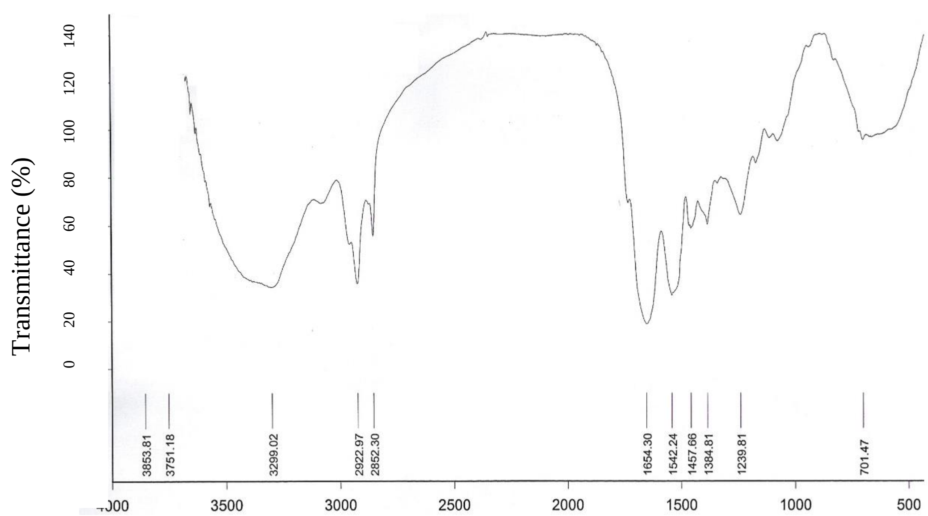

Figure 1- FT-IR spectrum of CFYM bio-absorbent

The XRD pattern (Figure 2a) did not show any specific peak. Therefore, it seems that no distinct mineral phase existed. Accordingly, CFYM has amorphous structure, which is expected for organic compounds. In SEM analysis, CFYM has a rough, bumpy and flex surface (Figure 2b and 2c). These images demonstrate some micro-pores on the adsorbent surface.

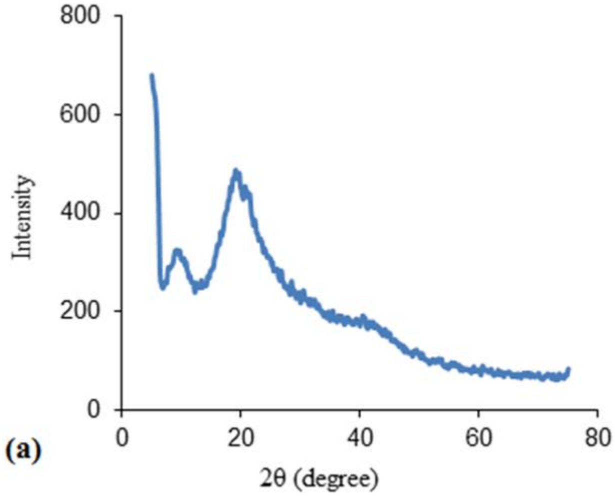

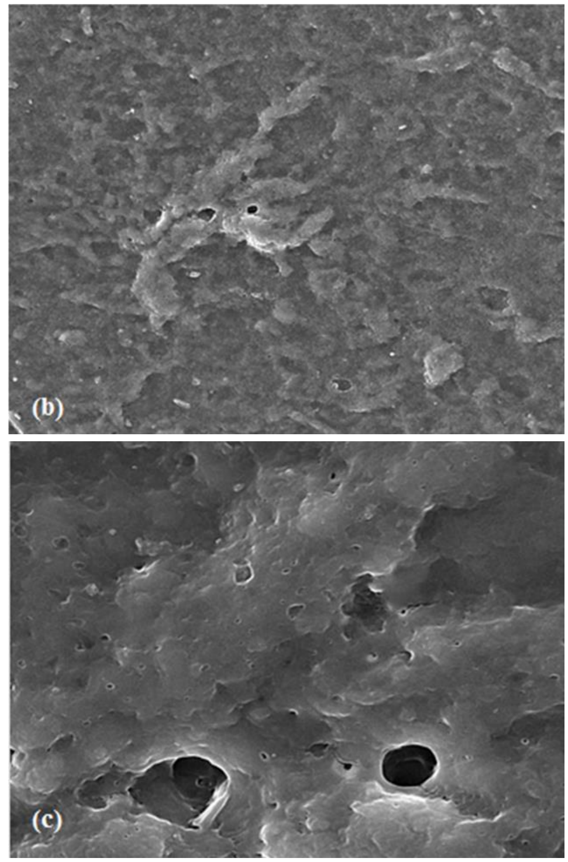

Figure 2- a) XRD pattern; b,c) SEM images of CFYM at different magnifications

Results of BET characterisation of CFYM are shown at Table 1. The specific surface area and pore volume were 3.430 $m^2\ g^{-1}$ and 0.007 $cm^3\ g^{-1}$, respectively. Average diameter of adsorbent pores was 8.7 nm. With regard to IUPAC classification [22], CFYM considered as mesoporous adsorbent. BET surface area of CFYM is comparable to those of other natural adsorbents such as soy meal hull (0.76 $m^2\ g^{-1}$) [23], ash gourd peel powder (0.48 $m^2\ g^{-1}$) [24], garden grass (21.20 $m^2\ g^{-1}$) [25], lentil shell (0.19 $m^2\ g^{-1}$) [26], olive stone (0.18 $m^2\ g^{-1}$) [27], rice shell (0.67 $m^2\ g^{-1}$) [28], and sunflower hull (6.05 $m^2\ g^{-1}$) [29].

Table 1. BET characteristics of CFYM

Characteristic	Unit	Value
BET surface area	$m^2\ g^{-1}$	3.4321
Total pore volume	$cm^3\ g^{-1}$	0.0075
Mean pore diameter	nm	8.7530

3.2. Optimization of effective variables on adsorption process

3.2.1. Effect of pH

As observed in Figure 3a, adsorption efficiency of MB on CFYM was improved from pH 2 to 10 and then decreased up to pH 12. This may be explained by negatively surface charge of CFYM adsorbent in alkaline pH. This is due to CFYM composition that includes collagen and proteins. Therefore, functional groups of amine, amide and carboxylic acids play significant role [30]. In contrast, there is interfering effect of OH^- at very high pH (more than 10) on anionic bio-adsorbent that impairs the process. Based on the results, pH=10 was selected as the best in terms of increased removal efficiency of MB.

3.2.2. Effect of adsorbent mass

As can be seen in Figure 3b, removal percent of MB from solution increased with increasing CFYM mass from 10 to 75 mg and then was constant. The improved adsorption efficiency by increasing the adsorbent mass is a result of developed surface area and active binding sites on the adsorbents that involved in MB interaction.

3.2.3. Effect of contact time

Removal effectiveness increased from 93% to 98% by extending the contact time from 10 to 50 min and then remained constant due to occupation of surface pores on adsorbent by MB (Figure 3c).

3.2.4. Effect of initial dye concentration

Amount of MB uptake by the adsorbent increased from 3.1 to 30.6 mg g^{-1} by increasing MB concentration from 10 to 100 mg l^{-1} (Figure 4). It might related to increased driving force, decreased diffusion resistance for cationic dye transfer and increased collision of MB and adsorbent.

3.2.5. Effect of temperature

According to Figure 3d, inhibitory effect of temperature on dye removal suggests that the adsorption process of MB on CFYM is exothermic. Similar result was observed by Lin et al. on basic dye removal by fly ash [31].

3.3. Equilibrium studies

Influence of dye initial concentration on adsorption capacity was monitored to find the adsorption isotherms. At this study, Langmuir, Freundlich, Tempkin and Dubinin-Radushkevich isotherms were followed [32–34]. Langmuir isotherm model associates with monolayer adsorption of adsorbate on adsorbent homogenous surface [32]. The linear equation of Langmuir isotherm is according to Eq. 3:

$$\frac{1}{q_e} = \frac{1}{(k_L\, q_m c_e)} + \frac{1}{q_m} \qquad \text{Eq. 3}$$

Where, C_e is equilibrium concentration of dye in solution (mg l^{-1}), q_e is equilibrium capacity of dye on the adsorbent (mg g^{-1}), q_m is maximum monolayer coverage of adsorbent (mg g^{-1}), k_L is Langmuir constant corresponds to the energy of adsorption (l mg^{-1}). R_L, separation factor, is a constant for describing the adsorption properties of Langmuir isotherm [35] which are derived from the following equation:

$$R_L = \frac{1}{1+ k_L\, c_o} \qquad \text{Eq. 4}$$

At this study, all R_L values were between 0.15 and 0.64 which shows that CFYM is appropriate adsorbent for MB removal [35] (Table 2, Figure 5).

Freundlich isotherm model refers to multilayer adsorption on heterogeneous surface according to Eq. 5:

$$\ln q_e = \ln k_F + \left(\frac{1}{n}\right) \ln c_e \qquad \text{Eq. 5}$$

Where, k_F is Freundlich constant ($mg^{1-(1/n)}\, g^{-1}\, L^{1/n}$), n is amount of deviation from linear region of the adsorption process and used to determine the adsorption type. The obtained value of n (n>1) indicated a desired physical adsorption process of MB on CFYM.

The Tempkin isotherm studies heat changes of adsorption [36] and the linearized equation is given as:

$$q_e = B \ln A + B \ln C_e \qquad \text{Eq. 6}$$

Where, B=RT/b and b is Tempkin isotherm constant (J mol^{-1}), A is quilibrium binding constant (l mg^{-1}) and B is constant correspond to heat of sorption.

The Dubinin-Radushkevich (D-R) isotherm provides energetic information on type of adsorption [37] and the linear equation is expressed in Eq. 7.

$$\text{Ln } q_e = \ln q_m - K_{DR}\, \varepsilon^2 \qquad \text{Eq. 7}$$

Where, q_e is amount of dye adsorbed per unite weight of adsorbent (mg g^{-1}), q_m is D-R adsorption capacity, K_{DR} is a constant correspond to adsorption energy (mol^2 J^{-2}) and ε is Polanyi potential which is given by following equation (Eq. 8):

$$\varepsilon = RT \ln\left(1 + \frac{1}{C_e}\right) \qquad \text{Eq. 8}$$

R^2, $K_{D\text{-}R}$ and q_m values of D-R isotherm are given in Table 2. Parameter E is defined as mean free energy of adsorption process for transferring one mole of adsorbate to adsorbent surface and its amount is calculated to evaluate the nature of adsorption process [38]. The value of E is calculated from Eq. 9.

$$E = \frac{1}{\sqrt{2K_{DR}}} \qquad \text{Eq. 9}$$

E value was calculated 1.11 kJ mol^{-1} that confirmed physical adsorption of MB on CFYM. The predicted plots of isotherms were observed in Figure 6a-d. Calculated parameters of the all studied isotherms are presented in Table 2. It seems that correlation coefficient (R^2) from Langmuir isotherm model was the highest among all isotherms. This result suggests that the experimental data fitted to the Langmuir model and monolayer adsorption of MB on the bio-adsorbent.

3.4. Kinetic studies

Various kinds of kinetic models were studied for MB adsorption on CFYM at ambient temperature. The linearized equation of pseudo-first-order kinetic is presented in Eq.10.

$$\log (q_e - q_t) = \log (q_e) - \frac{k_1 t}{2.303} \qquad \text{Eq. 10}$$

Where, q_e and q_t are amounts of the adsorbed dye on the adsorbent (mg g^{-1}) at equilibrium and certain time, respectively, and k_1 is adsorption rate coefficient of pseudo-first-order kinetic model (min^{-1}). Correlation coefficient of this isotherm model was 0.93 and significant difference of q_{exp} and q_{cal} showed that adsorption of MB on CFYM does not follow pseudo-first-order model.

In pseudo-second-order kinetic model, rate control is facilitated by chemical sorption [39]. The model is presented by Eq. 11 as follows.

$$\frac{t}{q_t} = \frac{1}{k_2 q_e^2} + \frac{t}{q_e} \qquad \text{Eq. 11}$$

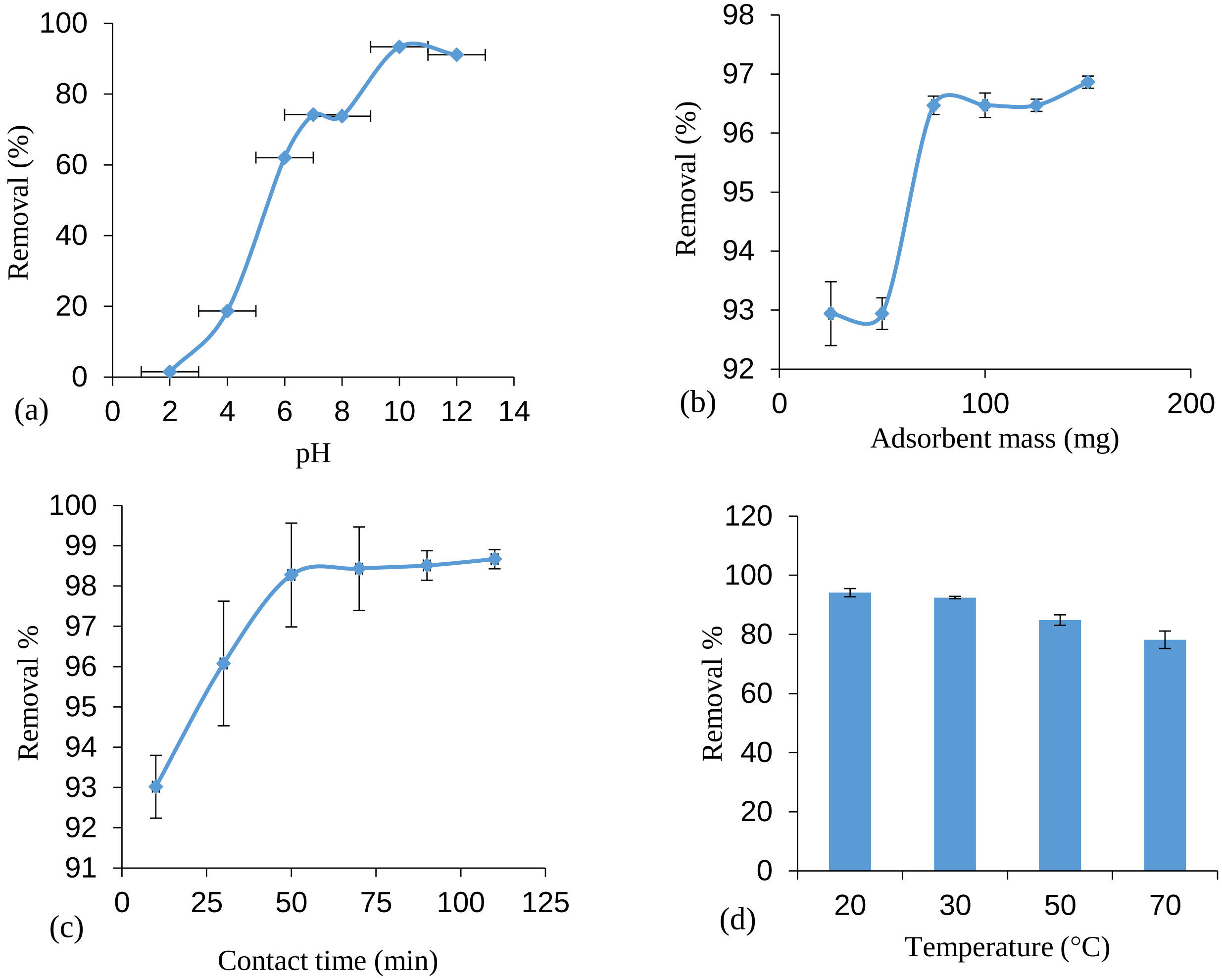

Figure 3- Effect of a) pH, b) adsorbent mass, c) contact time and d) temperature on adsorption of MB on CFYM

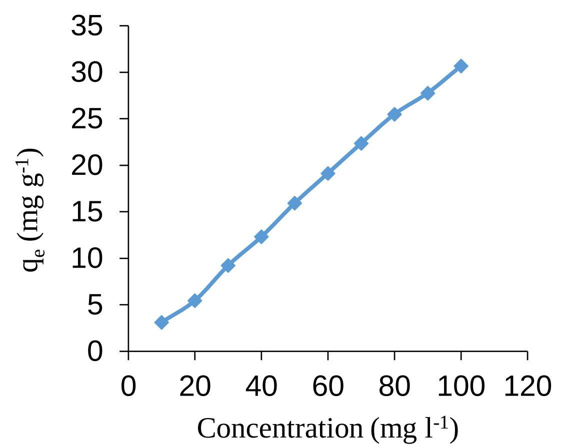

Figure 4- Effect of initial dye concentration on adsorption capacity of MB on CFYM surface

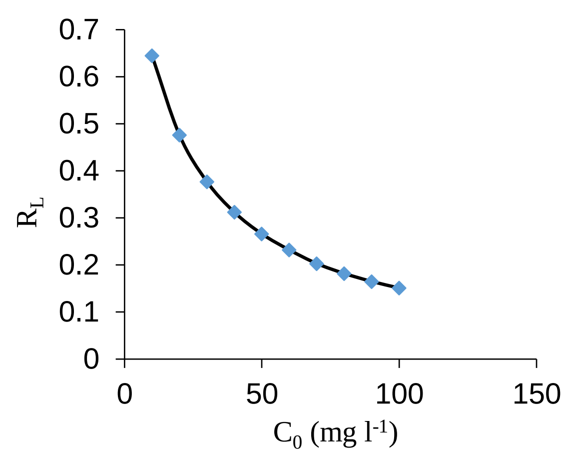

Figure 5- Values of obtained R_L for Langmuir isotherm

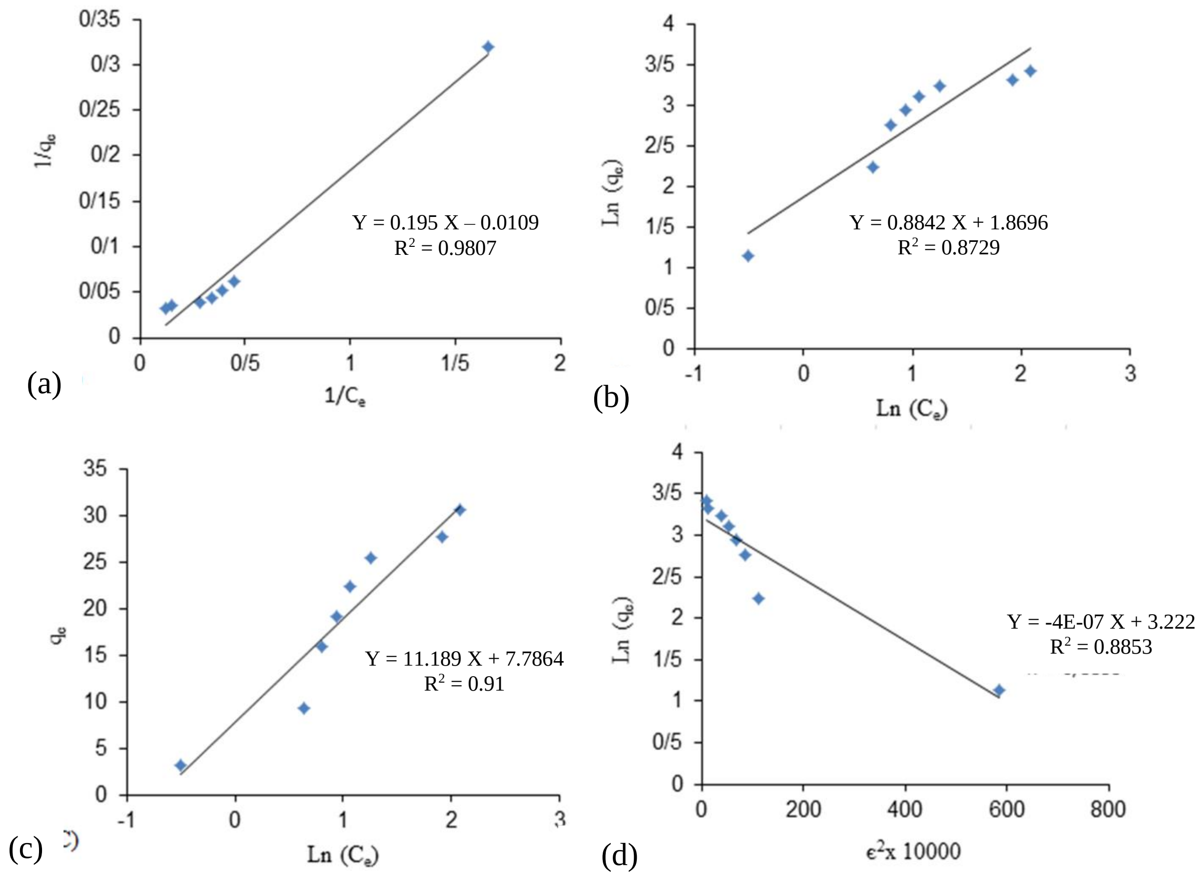

Figure 6- Plots of isotherms obtained for MB adsorption on CFYM: a) Langmuir, (b) Freundlich, c) Tempkin and d) Dubinin-Radushkevich isotherm models

Table 2. Isotherms parameters for adsorption of MB on CFYM

Isotherms	Parameters	Value
Langmuir	q_m (mg g^{-1})	91.740
$1/q_e = 1/(k_a q_m c_e) + 1/q_m$	K_a (l mg^{-1})	0.056
	R_L	0.151-0.645
	R^2	0.980
Freundlich	n	1.130
$\ln q_e = \ln k_F + (1/n)\ln c_e$	k_F (l mg^{-1})	4.740
	R^2	0.872
Tempkin	B	11.180
$q_e = B\ln\ (A) + B\ln\ (C_e)$	A (l mg^{-1})	1.780
	R^2	0.910
D-R	q'_m(mg g^{-1})	17.440
$\ln q_e = \ln q'_m - k_{DR}\varepsilon^2$	K_{DR} (mol^2 J^{-2})	4×10^{-7}
	E (kj mol^{-1})	1.118
	R^2	0.885

The excellent linear correlation with R^2=1 for t/q_t against t showed that the adsorption process of MB on CFYM is defined by a pseudo-second-order model (Figure 7b). It was further confirmed by slight difference between q_{cal} and q_{exp}.
Evaluated equation of intra-particle diffusion was proposed by Weber-Morris model [10] (Eq. 12):

$$q_t = k_{dif}\, t^{0.5} + C \qquad \text{Eq. 12}$$

Where, k_{dif} is rate constant (mg g^{-1} $min^{-0.5}$), and C is thickness of boundary layer (mg g^{-1}).
Elovich kinetic model is expressed in Eq. 13.

$$q_t = \frac{1}{\beta}\ln(\alpha\beta) + \frac{1}{\beta}\ln(t) \qquad \text{Eq. 13}$$

Where, α (mg g^{-1} min^{-1}) and β (g mg^{-1}) are rate constants for Elovich equation and show initial adsorption rate and desorption coefficient, respectively.
Kinetic parameters of the four models were calculated from slope and intercept of the plots and are presented in Table 3. As stated earlier, a good linearity and the highest correlation coefficient (R^2), was observed for pseudo-second-order model.

3.5. Thermodynamic study

Change of Gibbs free energy (ΔG^o, Kj mol^{-1}), enthalpy (ΔH^o, kJ mol^{-1}), and entropy (ΔS^o, kJ $mol^{-1}k^{-1}$) as thermodynamic indices were monitored to study the impact of thermal process on adsorption. Free energy change (ΔG°) as an effective parameter for spontaneity, is calculated by the following equations (Eq. 14 and 15) [40].

$$\Delta G^\circ = \Delta H^\circ - T\Delta S^\circ \qquad \text{Eq. 14}$$

$$\Delta G^\circ = -RT\ln k_c \qquad \text{Eq. 15}$$

Where, R is gas constant (8.314 J mol^{-1} K^{-1}), T is temperature (°K) and k_c (l mol^{-1}) is thermo-dynamic equilibrium constant that could be determined by following equation (Eq. 16).

$$K_{(c)} = \frac{q_e}{C_e} \qquad \text{Eq. 16}$$

$$\ln(k_c) = -\frac{\Delta H^\circ}{RT} + \frac{\Delta S^\circ}{R} \qquad \text{Eq. 17}$$

ΔH^o and ΔS^o are obtained from slope and intercept of ln k vs. 1/T plot (Figure 8). Amounts of ΔG^o, ΔH^o and ΔS^o are presented in Table 4.
The negative enthalpy confirmed that the adsorption process is exothermic. ΔG^o was positive by increasing the temperature from 20 °C to 70°C, which revealed the spontaneous nature of adsorption process. Furthermore, the negative ΔS^o was correlated to a decreased randomness at adsorbent-solution interface in the process.

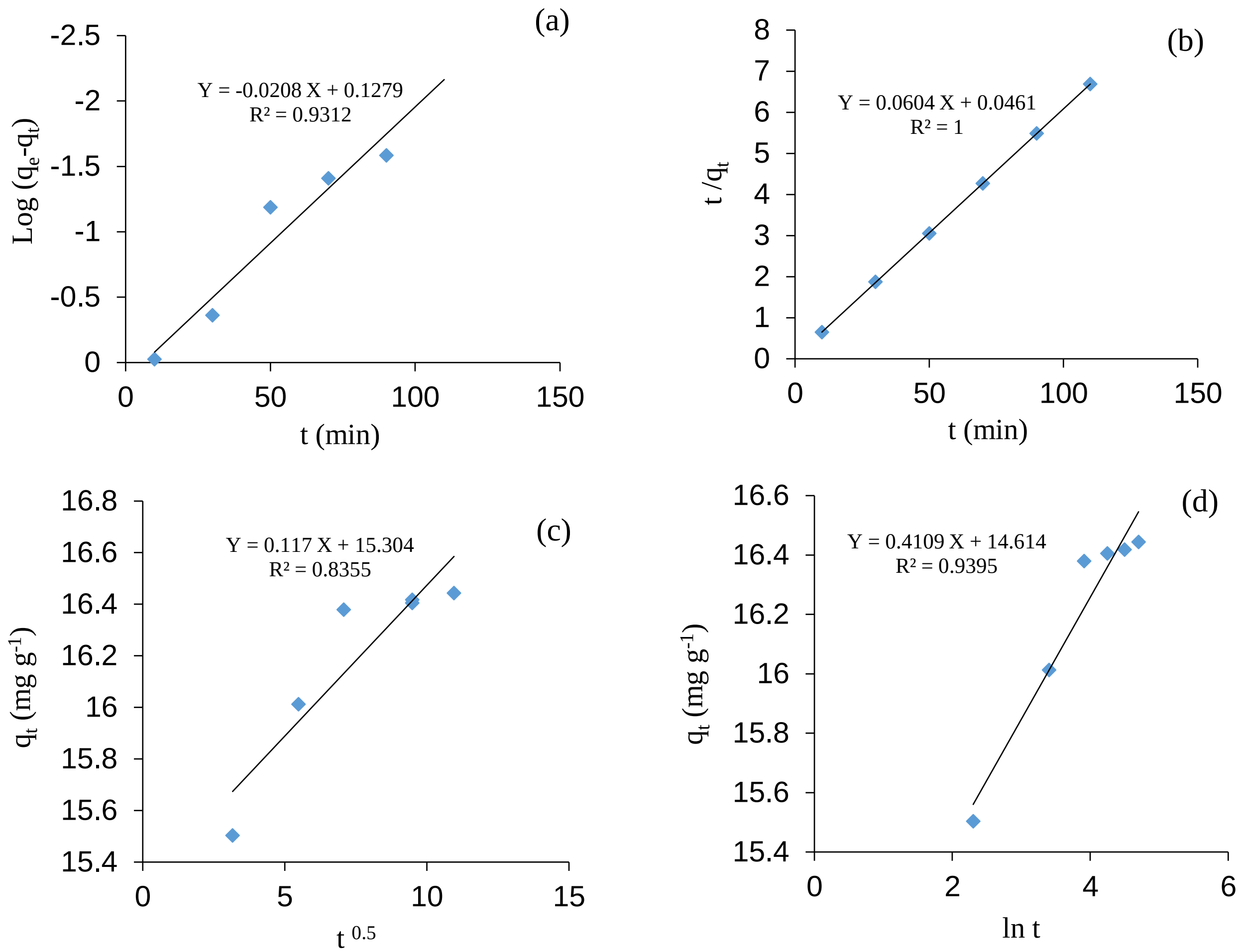

Figure 7- Kinetic modeling of adsorption of MB on CFYM; a) pseudo-first-order, b) pseudo-second-order, c) intra-particle diffusion, d) Elovich kinetic models

Table 3. Kinetic parameters for adsorption of MB on CFYM

Model	Parameters	Value
Pseudo-first order	$q_{e,exp}$ (mg g^{-1})	16.400
$\log(q_e - q_t) = \log q_e - k_1 t / 2.303$	q_e (mg g^{-1})	1.342
	K_1 (min^{-1})	0.047
	R^2	0.931
Pseudo second order	q_e (mg g^{-1})	16.550
$t / q_t = 1 / k_2 q_e^2 + t / q_e$	K_2 (mg l^{-1} min^{-1})	0.079
	R^2	1
Intra-particle diffusion	C	15.304
$q_t = k_{dif} t^{0.5} + C$	K_{dif} (mg g^{-1} min$^{-0.5}$)	0.117
	R^2	0.835
Elovich	α (mg g^{-1} min^{-1})	3×10^{12}
$q_t = 1/\beta \ln(\alpha\beta) + 1/\beta \ln\ (t)$	β (g mg^{-1})	2.433
	R^2	0.939

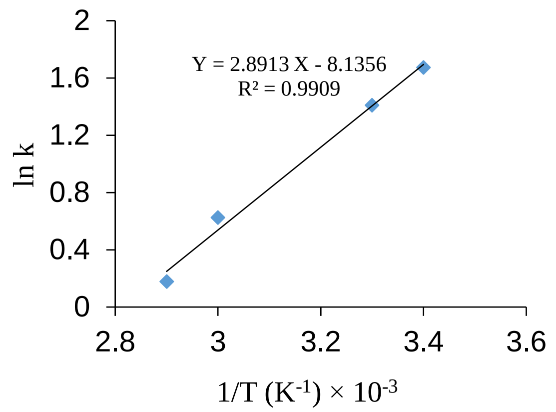

Figure 8- Effect of temperature on adsorption kinetics of MB on CFYM

Table 4- Thermodynamic indices for adsorption of MB on CFYM

ΔG°(kJ mol $^{-1}$)				ΔH° (J mol $^{-1}$)	ΔS° (J mol $^{-1}$ k $^{-1}$)
20°C	30°C	50°C	70°C		
-19.842	6.016	7.778	9.616	-24.038	-67.639

4. Conclusion

At this study, a novel, available, inexpensive and natural bio-adsorbent was prepared and further used for organic pollutants removal from aqueous environments. Isotherm, kinetic and thermo-dynamic analysis were conducted. As a result, the equilibrium data were best-fitted to Langmuir isotherm and revealed a monolayer coverage of CFYM by MB. In addition, the process followed pseudo-second-order kinetic model. Some advan-tages such as the simple process, and safety, low cost, biodegradability, and availability of the bio-adsorbent make it superior to the chemical adsorbents for waste removal purposes.

5. Acknowledgment

The authors would like to acknowledge the Research Council of Shahid Madani University for its financial support to the current work.

6. Conflict of interest

The authors have declared no conflict of interest.

References

1. Labanda J, Sabate J, Liorens J. Modelling of the dynamic adsorption of an anionic through ion-exchange membrane adsorber. J Membr Sci. 2009; 340: 234–240. https://doi.org/10.1016/j.memsci.2009.05.036.

2. Santhy K, Selvapathy P. Removal of reactive dyes from wastewater by adsorption on coir pith activated carbon. Bioresour Technol. 2006; 97: 1329–1336. https://doi.org/10.1016/j.biortech.2005.05.016.

3. Yang J, Qiu K. Preparation of activated carbons from walnut shells via vacuum chemical activation and their application for methylene blue removal. Chem Eng J. 2010; 165: 209–217. https://doi.org/10.1016/j.cej.2010.09.019.

4. Turabik M. Adsorption of basic dyes from single and binary component systems onto bentonite: simultaneous analysis of basic red 46 and basic yellow 28 by first order derivative spectrophotometer analysis method. J Hazard Mater. 2008;158: 52–64. https://doi.org/10.1016/j.jhazmat.2008.01.033.

5. Gupta VK, Suha S. Application of low cost adsorbents for dye removal-a review. J Environ Manage. 2009; 90: 2313–2342. https://doi.org/10.1016/j.jenvman.2008.11.017.

6. Purkait MK, Maiti A, Dasgupta S, De S. Removal of congo red using activated carbon and its regeneration. J Hazard Mater. 2007;145: 287-295. https://doi.org/10.1016/j.jhazmat.2006.11.021.

7. Ji L, Shao Y, Xu Z, Zheng S, Zhu D. Adsorption of Monoaromatic Compounds and Pharmaceutical Antibiotics on Carbon Nanotubes Activated by KOH Etching. Environ Sci Technol. 2010; 44: 6429–6436. https://doi.org/10.1021/es1014828.

8. Khosravi M, Azizian S. Adsorption of anionic dyes from aqueous solution by iron oxide nanosphere. J Ind Eng Chem. 2014; 20: 2561–2567. https://doi.org/10.1016/j.jiec.2013.10.040.

9. Panie VV, Seslija SI, Nesic AR, Veliekovie SJ. Adsorption of azo dyes on polymer materials. Hem Ind. 2013; 67: 881–900. https://doi.org/10.2298/HEMIND121203020P.

10. Qin QD, Ma J, Liu K. Adsorption of anionic dyes on ammonium-functionalized MCM-41. J Hazard Mater. 2009; 162: 133-139. https://doi.org/10.1016/j.jhazmat.2008.05.016.

11. Annadurai G, Juang RS, Lee DJ. Use of cellulose based wastes for adsorption of dyes from aqueous solutions. J Hazard Mater. 2002;92: 263–274. https://doi.org/10.1016/s0304-3894(02)00017-1.

12. Salleh MAM, Mahmoud DK, Abdul Karim WAW, Idris A. Cationic and anionic dye adsorption by agricultural solid wastes: a comprehensive review. Desalination. 2011; 280: 1–13. https://doi.org/10.1016/j.desal.2011.07.019 2.

13. Kamrani M, Akbari A, Yunessnia lehi A. Chitosan-modified acrylic nanofiltration membrane for efficient removal of pharmaceutical compound. J Environ Chem Eng. 2018; 6: 583–587. https://doi.org/10.1016/j.jece.2017.12.044.

14. Acosta R, Nabarlatz D, Sanchez-Sanchez A, Jagiello J, Gadonneix P, Celzard A, Fierro V. Adsorption of Bisphenol A on KOH-activated tyre pyrolysis char. J Environ Chem Eng. 2018; 6: 823–833. https://doi.org/10.1016/j.jece.2018.01.002.

15. Bhattacharyya KG, Sharma A. Azadirachta indica leaf powder as an effective biosorbent for dyes: a case study with aqueous congo red solutions. J Environ Manage. 2004; 71: 217–229. https://doi.org/10.1016/j.jenvman.2004.03.002.

16. Ali H. Biodegradiation of synthetic dyes- a review. Water Air Soil Pollut. 2010; 213: 251–273. https://doi.org/10.1007/s11270-010-0382-4.

17. Umoren SA, Etim UJ, Israe AUJ. Adsorption of methylene blue from industrial effluent using poly (vinyl alcohol). Mater Environ Sci. 2012; 4: 75–86.

18. Latif MM, Ibrahim AM, El-Kady MF. Adsorption Equilibrium, kinetics and thermodynamics of methylene blue from aqueous solutions using biopolymer oak sawdust Composite. Am J Sci. 2010; 6: 267–283.

19. Farrokhzadeh S, Razmi H. Use of chicken feet yellow membrane as a biosorbent in miniaturized solid phase extraction for determination of polycyclic aromatic hydrocarbons in several real samples. Microchem J. 2018; 142: 403-410. https://doi.org/10.1016/j.microc.2018.06.036.

20. Dos SK, Guha AK. Biosorption of chromium by Termitomyces clypeatus. Colloids Surf B. 2007; 60: 46–54. https://doi.org/10.1016/j.colsurfb.2007.05.021.

21. Cheng XZ, Hu CJ, Cheng K, Wei BM, Hu SC. Removal of Mercury from Wastewater by Adsorption Using Thiol-Functionalized Eggshell Membrane. Adv Mat Res. 2010; 113−114: 22−26. https://doi.org/10.4028/www.scientific.net/AMR.113-116.22

22. Sing KSW, Everett DH, Haul RAW, Moscou L, Pierotti RA, Rouquerol J, Siemieniewska T. Reporting physisorption data for gas/solid systems with special reference to the determination of surface area and porosity. Pure Appl Chem. 1985; 57: 603–619. https://doi.org/10.1351/pac198557040603.

23. Arami M, Limaee NY, Mahmoodi NM, Tabrizi NS. Equilibrium and kinetics studies for the adsorption of direct and acid dyes from aqueous solution by soy meal hull. J Hazard Mater. 2006; 135: 171–179. https://doi.org/10.1016/j.jhazmat.2005.11.044.

24. Sreenivas KM, Inarkar MB, Gokhale SV, Lele SS. Re-utilization of ash gourd (Benincasa hispida) peel waste for chromium(VI) biosorption: equilibrium and column studies. J Environ Chem Eng. 2014; 2: 455–462. https://doi.org/10.1016/j.jece.2014.01.017.

25. Hossain MA, Ngo HH, Guo WS, Setiadi T. Adsorption and desorption of copper(II) ions onto garden grass. Bioresour Technol. 2012; 121: 386–395. https://doi.org/10.1016/j.biortech.2012.06.119.

26. Aydın H, Bulut Y, Yerlikaya C. Removal of copper (II) from aqueous solution by adsorption onto low-cost adsorbents. J Environ Manage. 2008; 87: 37–45. https://doi.org/10.1016/j.jenvman.2007.01.005.

27. Fiol N, Villaescusa I, Martínez M, Miralles N, Poch J, Serarols J. Sorption of Pb(II), Ni(II), Cu(II) and Cd(II) from aqueous solution by olive stone waste. Sep Purif Technol. 2006; 50: 132–140. https://doi.org/10.1016/j.seppur.2005.11.016.

28. Ahmaruzzaman M, Gupta VK. Rice husk and its ash as low-cost adsorbents in water and wastewater treatment. Ind Eng Chem Res. 2011; 24: 13589–13613. https://doi.org/10.1021/ie201477c.

29. Witek-Krowiak A. Analysis of temperature-dependent biosorption of Cu^{2+} ions on sunflower hulls: kinetics, equilibrium and mechanism of the process. Chem Eng J. 2012; 192: 13–20. https://doi.org/10.1016/j.cej.2012.03.075.

30. Yi F, Guo ZX, Zhang LX, Yu J, Li Q. Soluble eggshell membrane protein: preparation, characterization and biocompatibility. Biomaterials. 2004; 25: 4591‒4599. https://doi.org/10.1016/j.biomaterials.2003.11.052.

31. Lin JX, Zhan SL, Fang MH, Qian XQ, Yang H. Adsorption of basic dye from aqueous solution onto fly ash. J Environ Manage. 2008; 87: 193–200. https://doi.org/10.1016/j.jenvman.2007.01.001.

32. Dogan, M.; Karaoglu, M.H.; Alkan, M. (2009) Adsorption kinetics of maxilon yellow 4GL and maxilon red GRL dyes on kaolinite. J Hazard Mater. 165: 1142–1151. https://doi.org/10.1016/j.jhazmat.2008.10.101.

33. Abdelwahab O. Evaluation of the use of loofa activated carbons as potential adsorbents for aqueous solutions containing dye. Desalination. 2008; 222: 357–367. https://doi.org/10.1016/j.desal.2007.01.146.

34. Kargi F, Ozmıhcı S. Biosorption performance of powdered activated sludge for removal of different dyestuffs. Enzyme Microb Technol. 2004; 35: 267–271. https://doi.org/10.1016/j.enzmictec.2004.05.002.

35. Vimonses V, Lei S, Jin B, Chow CWK, Saint C. Kinetic study and equilibrium isotherm analysis of Congo Red adsorption by clay materials. Appl Clay Sci. 2009; 43: 465–72. https://doi.org/10.1016/j.cej.2008.09.009.

36. Nadeem R, Nasir MH, Hanif MS. Pb (II) sorption by acidically modified Cicer arientinum biomass. Chem Eng J. 2009; 150: 40–48. https://doi.org/10.1016/j.cej.2008.12.001.

37. Menger FM, Markazi M, Mahmoodi NM, Nikkor H, Tehrani-Bagha AR. The sorption of cationic dyes onto kaolin: Kinetic, isotherm and thermodynamic studies. Desalination. 2011; 266: 247–80. https://doi.org/10.1016/j.desal.2010.08.036.

38. Demiral H, Demiral I, Tümsek F, Karabacakoğlu B. Adsorption of chromium(VI) from aqueous solution by activated carbon derived from olive bagasse and applicability of different adsorption models. Chem Eng J. 2008; 144: 188–196. https://doi.org/10.1016/j.cej.2008.01.020.

39. Haddad EI, Slimani R, Mamouni R, Laamari MR, Rafqah S, Lazar S. Evaluation of potential capability of calcined bones on the biosorption removal efficiency of safranin as cationic dye from aqueous solutions. J Taiwan Inst Chem Eng. 2013; 44: 13–18. https://doi.org/10.1016/j.jtice.2012.10.003.

40. Oladoja NA, Ahmad AL. Gastropod shell as a precursor for the synthesis of binary alkali-earth and transition metal oxide for Cr(VI) Abstraction from Aqua System. Sep Purif Technol. 2013; 116: 230–239. https://doi.org/10.1016/j.seppur.2013.05.042